Scientific African 17 (2022) e01329

Contents lists available at ScienceDirect

Scientific African

journal homepage: www.elsevier.com/locate/sciaf

Comparative study between TIG-MIG Hybrid, TIG and MIG welding of 1008 steel joints for enhanced structural integrity

Cynthia Samuel Abima[a,*], Stephen Akinwale Akinlabi[b], Nkosinathi Madushele[a], Esther Titilayo Akinlabi[c]

[a] Department of Mechanical Engineering Science, University of Johannesburg, Johannesburg, South Africa
[b] Department of Mechanical Engineering, Walter Sisulu University, Butterworth, South Africa
[c] Pan African University for Life and Earth Sciences Institute, Ibadan, Nigeria

ARTICLE INFO

Article history:
Received 15 September 2021
Revised 27 June 2022
Accepted 12 August 2022

Editor DR B Gyampoh

Keywords:
Hardness
Microstructure
Structural integrity
TIG-MIG hybrid
Tensile strength
Welding

ABSTRACT

This study investigates the combined effect of the Tungsten Inert Gas (TIG) and Metal Inert Gas (MIG) arcs in achieving improved mechanical and microstructural properties compared with the standalone TIG and MIG arcs based on optimum parameters setting for the TIG and MIG welding processes. TIG and MIG Miller welding machines with a maximum capacity of 400 A were used as the combined heat source. The welds produced by the TIG-MIG, TIG and MIG welding processes were characterized via tensile and hardness testing, macrostructural investigations, microstructural analysis, and X-ray diffraction analysis. The results from the characterization show that the TIG-MIG hybrid joint had better tensile strength, yield strength and percentage elongation properties than the standalone MIG and TIG welded joints, respectively. The fractograph of the TIG-MIG joint was characterized with uniform fine dimples showing a more ductile failure characteristic. Macrostructural evaluation revealed that the heat-affected zone of the TIG-MIG hybrid joint was larger than those of the individual TIG and MIG processes. The microstructure of the TIG-MIG joint showed an abundant presence of acicular ferrite with cementite on the boundaries of ferrite grain. Martensite phases diffracted at higher intensity peaks in the TIG weld while iron phases diffracting at high-intensity peaks in the MIG weld, and lastly, the TIG-MIG welded joint showed only iron phases which accounted for its lowest hardness value when compared with standalone MIG and TIG joints.

Introduction

The adoption of combined arc welding processes such as double electrode gas metal inert gas welding (DE- GMAW), tandem tungsten inert gas welding, tandem gas metal inert gas welding and TIG-MIG hybrid welding has increasingly gained more attention owing to the ability to improve weld properties. The tandem TIG welding technique developed by Qin et al. [1] resulted in satisfactory quality welds. But this technique was of low heat input and low metal deposition rate leading

* Corresponding author.
E-mail address: oyamacynthia@gmail.com (C.S. Abima).

https://doi.org/10.1016/j.sciaf.2022.e01329

to low productivity. The pulsed tandem GMAW process developed by Chen et al. [2] overcame the low deposition rate problem associated with the tandem TIG welding. However, as this process required an oxidizing atmosphere for shielding the weld pool, it was not suitable for joining high strength steel. Improve deposition rate was also achieved by employing the DE-GMAW. However, the process required a special circuit arrangement. The aforementioned combined arc processes still had deficiencies associated with the conventional TIG and MIG processes, especially in weld pool behavior and bead formation. Consequently, Kanemaru et al. [3] invented the TIG-MIG hybrid welding method, which simultaneously combines the high-quality and high-efficiency attributes of the respective TIG and MIG welding processes in improving weld quality as appraised by Zhou et al. [4]. The TIG-MIG welding process is efficient as it does not require special circuit and unique power source properties, as highlighted by Zong et al. [5]. The TIG and MIG arcs can be combined such that the TIG arc is leading while the MIG arc is trailing written as TIG-MIG or the MIG arc leading while the TIG arc trailing written as MIG-TIG hybrid welding. Kanemaru et al. [6] alluded that the additional TIG arc stabilizes the MIG arc even when pure argon gas is used for shielding. Following this, Ding et al. [7] highlighted that the TIG-MIG hybrid process was capable of welding dissimilar magnesium and ferritic stainless steel due to arc stability. Besides obtaining a stable MIG arc that promotes good weld bead formation for similar and dissimilar metal welds, Cheng et al. [8] reported strong joint connections between copper and stainless steel plates joined by MIG-TIG double-sided arc welding method.

Recent studies have established the improved structural integrity of the TIG-MIG hybrid welding process compared with the standalone techniques. Despite this advantage of the hybrid welding method, few authors have compared the evolved properties of the TIG and MIG hybrid joints against the conventional standalone TIG and MIG joints. For instance, Ye et al. [9] compared the microstructural and mechanical properties of aluminium/carbon steel joint produced by MIG-TIG double-sided arc welding-brazing (DSAWB) with the conventional MIG welding process. The authors reported that the tensile strength of the MIG-TIG process was two and half times that of the conventional MIG process. It was also noted that the MIG-TIG process required less heat input to produce a good weld bead, especially at the backside of the weld compared to that required to produce the same effect using the conventional MIG process. It is also important to highlight that the lower heat input characteristic of the combined process limited the thickness of the intermetallic compound formed in the MIG-TIG weld, which favoured the joint strength. The intermetallic thickness of the combined process was reported to be 2.03 μm in comparison with 4.20 μm thickness for the conventional MIG process. Similarly, Chen et al. [10] investigated the influence of low current auxiliary TIG arc on the microstructure and weld bead formation of mild steel joints during TIG-MIG hybrid welding and compared the result with the standalone MIG joints. The authors reported that a leading TIG arc stabilizes the trailing MIG arc and decentralizes the MIG arc force in the TIG-MIG hybrid process, which causes a reduction in the impingement of molten droplets and the deceleration of backward fluid flow. The authors claim that the deceleration of the backward flow provided more time for the molten metal to fill the weld toe, resulting in suppression of the undercut defect, leading to better weld formation compared to the standalone MIG process. It was observed that the weld zone's width of the TIG-MIG process was greatly reduced compared to that obtained from the conventional MIG welding process and the microstructural grains of the hybrid process did not deteriorate despite the increase in heat input in the hybrid process. Zhou et al. [4] also achieved an ideal front and back weld bead for 24 mm thick mild steel plates by the MIG-TIG hybrid process without using backing plates. The combined arc interaction was said to have improved the heat distribution at the root weld because the additional TIG arc introduces more heat at the bottom of the weld bead, leading to complete fusion. The author reported that during the MIG-TIG process, adjusting the MIG and TIG welding current, the distance between the two arcs, the torch angles of the two arcs, a sound weld shape and complete penetration can be realized.

Furthermore, Zhang et al. [11] compared the weld formation and tensile strength of the double-sided TIG-MIG joint with the standalone MIG joint of aluminium/titanium produced with the same heat input value. Their result showed that the TIG-MIG double-sided joint had better weld formation and tensile strength than the standalone MIG joint. Additionally, the mechanical properties of stainless steel/mild steel joints produced by the TIG-MIG welding process, TIG welding process, and MIG welding process were also investigated by Ismail et al. [12]. The welds obtained from the three welding processes were characterized based on their mechanical integrities accessed from the respective percentage elongation, the tensile strengths, the percentage reduction in area, and the yield strengths. Their result shows that the TIG-MIG welded joint was only best in yield strength, while the TIG welded joint had superior tensile strength, percentage elongation, and percentage reduction in area than those produced by the TIG-MIG welding process. Sahasrabudhe and Raut [13] reported a higher impact strength, higher average metal deposition rate and 58% increase in productivity of the TIG-MIG hybrid process compared to the conventional MIG process. Zong et al. [5] and Meng et al. [14] observed that the welding speed of the TIG-MIG process was faster than that of the conventional MIG welding process.

Although the TIG-MIG hybrid process improves weld quality and can increase dynamic load capacity and fatigue strength compared to the conventional MIG counterpart, as predicted by Chen et al. [10]. The process parameters adopted for the TIG and MIG processes in the present studies were not selected according to any experimental design approach. Consequently, the hybrid joints produced from the interaction of the two arcs may not meet industrial/structural standards even if they show improved properties compared to the standalone MIG and TIG processes. A random selection and adoption of input parameters may lead to weak joints with poor mechanical and microstructural properties.

Moreso, The work of Zhou et al. [4] and Ismail et al. [12] suggest that optimizing the parameters of the MIG and TIG welding processes will aid in achieving improved properties for the TIG-MIG hybrid process. Hence, for better weld integrity of the TIG-MIG hybrid process, it becomes imperative to employ suitable welding process parameters for the TIG and MIG

welding processes. Therefore, this study performed a comparative analysis on the evolved properties of the TIG-MIG, TIG, and MIG welding processes based on optimum sets of TIG and MIG welding parameters for the enhanced structural integrity of the TIG-MIG hybrid process for typical industrial applications. To the best of our knowledge, this approach has not been adopted in any study so far. This study approach helped to ascertain the integrity of the TIG-MIG hybrid process over the conventional standalone TIG and MIG welding processes.

Experimental details

Materials and equipment

In this experiment, a Miller 400 A direct current electrode positive (DCEP) MIG welding machine and a Miller 400 A direct current electrode negative (DCEN) TIG machine were used in producing the welds. A 3.2 mm diameter tungsten electrode and 2.4 mm diameter ER70S/6 carbon filler rod were used as wire electrode and filler material. The TIG arc was shielded with the crystal argon gas, while the MIG arc was shielded with a gas mixture of Argon + O_2 + CO_2. The welding material was 1008 mild steel of 6 mm thickness. The elemental composition by weight of the material is Fe - 99.58, C - 0.079, S - 0.0098, Mn - 0.32, and P - 0.0098.

Procedures

Butt joint configuration was adopted for this study. The individual MIG and TIG joints were produced with the machine specification described in section 2.1. The schematic of the TIG- MIG hybrid method is shown in Fig. 1. The TIG torch proceeded the MIG torch, and the welding was done in the direction normal to the rolling of the plates.

Prior to welding, the plates were freed from impurities by removing oxide scales from the surface of the plates and cleaning with acetone. Butt welding experiments were conducted under the optimized parameters to study and compare the mechanical and microstructural properties of the welded joints. Smaller sets of specimens were cut from the welded plates and prepared according to standard metallographic procedures for microstructural analysis. Test specimens for mechanical characterization were also machined according to standard tensile and hardness specifications. The Scanning Electron Microscopy (SEM) and the Ultima IV X-ray diffractometer were used to analyse the joints' fracture morphology and phase composition, respectively.

Process parameters

With weld integrity in mind, the study employed optimum parameters settings of the TIG and MIG welding processes on the criteria of larger is better for the tensile strength based on the Taguchi L-9 orthogonal matrix. The input parameters selected in this study for the three welding processes are the welding current, welding voltage and the gas flow rate. The levels of input parameters for the TIG welding process were voltage −10,15,20, Current −140,160,180, gas flow rate −15, 17, 19. The levels of input parameters for the MIG welding process were voltage - 20,25,30, Current - 220, 250, 280, gas flow

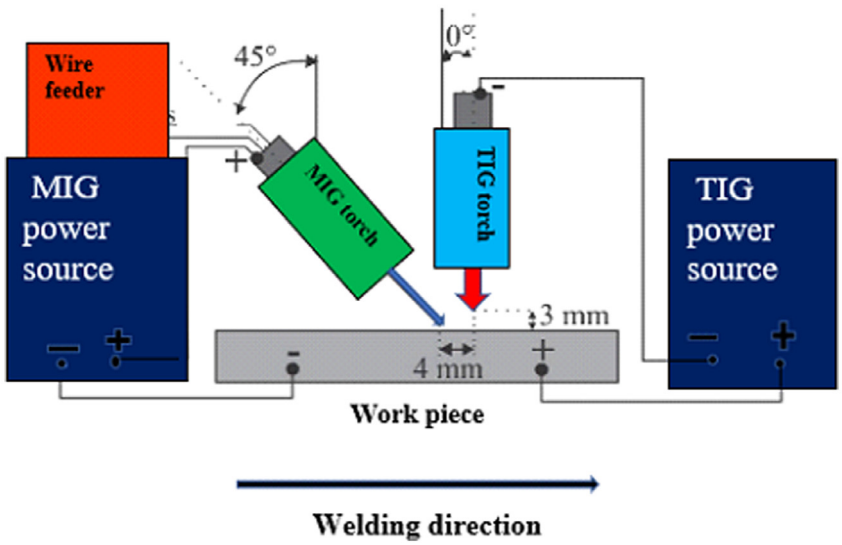

Fig. 1. The schematic of the TIG- MIG hybrid method.

Table 1
Welding parameters.

Type of Welding	Electrode connection	Welding Voltage (V)	Welding Current (A)	Gas flow rate(L/mm)
TIG	DCEN	15	180	15
MIG	DCEP	30	280	17
TIG-MIG	DCEN/DCEP	15/30	180/280	15/17

rate - 15, 17, 19. The optimum welding parameters obtained for each welding process after optimization and used in this study are presented in Table 1.

Experimental results

Tensile properties and fracture morphology

The tensile properties of the welds produced by the TIG, MIG and TIG-MIG welding processes were evaluated. Three replicate specimens were tested for each weld type, and the average values were obtained. All the welded joints failed at the parent material region, indicating that the weld joints were stronger than the parent material [15], which is industrially accepted. Fig. 2 shows the fractured specimens for the three weld types.

A comparative stress-strain plot for one out of the three replicates specimens for each welding type is presented in Fig. 3. The tensile properties for the three welding processes and the parent material are presented in Table 2.

Fig. 2. Fractured specimens (a) TIG joint (b) MIG joint (d) TIG-MIG joint.

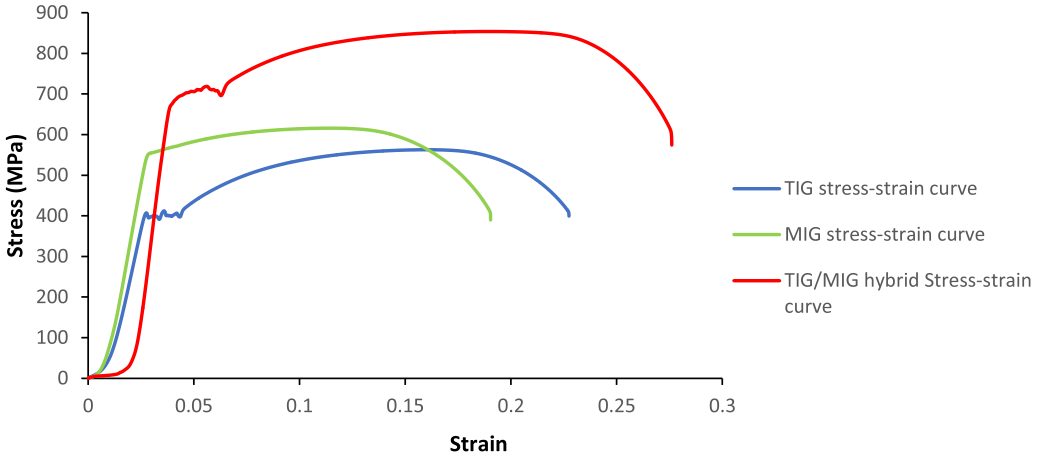

Fig. 3. Stress-strain curve for TIG, MIG and TIG-MIG welding processes.

Table 2
Tensile test results.

Welding type	Ultimate Tensile strength (MPa)	Yield strength (MPa)	Percentage Elongation (%)	Joint efficiency (%)	Heat input (J/mm)	Welding Speed (mm/min)
TIG	476.6	322	24.1	117.4	3780	30.0
MIG	613.3	501.9	21.9	151.1	675.36	597
TIG-MIG hybrid	851	686.1	25.9	209.9	4620	
PM	406.5	313.4	42			

Table 3
Parameters of weld bead Geometry of TIG, MIG and TIG-MIG hybrid joints.

Type Welding	Width of weld bead (mm)	Reinforcement height (mm)	Width of Heat-affected zone (mm)	Fusion area (mm^2)
TIG	4.791	Nill	1.261	6.848
MIG	5.430	0.407	1.060	8.361
TIG-MIG hybrid	5.119	1.050	1.632	9.182

The result of the tensile test shows that the TIG-MIG hybrid joint had better tensile strength, yield strength and percentage elongation compared to the standalone MIG and TIG welded joints. The MIG welded joint showed better tensile strength and yield strength compared to the TIG welded joint. However, the percentage elongation of the TIG welded joint was higher than that of the MIG welded joint. The tensile strength of the joints determines the load-carrying capacity of the weldments, and the yield strength determines the limit below which failure will not occur. It is worthy to state that although the heat input during the TIG-MIG hybrid process was more than those of the individual TIG and MIG Processes, the tensile properties did not deteriorate.

Fig. 4 shows the SEM fractograph together with the EDS scan. It is observed that the fracture modes for the joints are different. The TIG weld is characterized by coarse dimples surrounded by small size dimples. Large tearing ridges (indicted by the red arrow) and cleavage fracture indicate a brittle fracture mode in the MIG welds. The brittle mode of fracture may be attributed to the presence of oxide and impurities as seen in the EDS scan . The fractograph of the TIG-MIG joint is characterized by uniform fine dimples showing a ductile failure.

Hardness properties

The Vickers hardness distribution for the three welding processes (TIG, MIG and TIG-MIG hybrid) is illustrated in Fig. 5.

The hardness profile reveals that the fusion zones of the weldments had higher hardness values than the heat-affected zones and the base material for the three weld types. The microhardness profiling also shows that the TIG welded joint had the highest hardness property. The hardness of the MIG weld is also seen to be higher than that of the TIG-MIG hybrid process. The higher hardness values of the TIG and MIG joints are attributed to the presence of martensite phases, as seen from the diffractogram obtained from the XRD analysis. The TIG-MIG hybrid revealed only iron phases accounting for the lower hardness property than the standalone TIG and MIG processes.

Macrostructure and microstructure

Macrostructural and microstructural evolution occur during and after welding processes. These evolved properties determine the quality of the welds and the reliability of the weldments for structural members. The macrographs (Fig. 6) reveals full penetration joints produced by all three welding processes. The welds were free from cracks and pores. The width of the weld bead, the width of the heat-affected zone, the fusion areas of the three welding processes are seen to be different. The different weld types, input parameters, heat input, and welding speed accounts for the differences in the geometries. However, the shapes of the three weld types are somewhat similar.

The dimensions of the width of the weld bead, the width of the heat-affected zone, the fusion area and the heights of reinforcement are measured by the ImageJ software and presented in Table 3

The MIG weld bead is much larger than those obtained from the TIG and TIG-MIG joints. This is due to the higher levels of the input parameters combination. The fusion area of the TIG-MIG hybrid welded joint (9.182 mm^2) is larger than those of the TIG (6.848 mm^2) and MIG (8.361mm^2). The TIG-welded joint had the lowest fusion area.

The width of the heat-affected zone of the TIG-MIG hybrid joint is also seen to be larger than those of the TIG and MIG processes. This is a result of the relatively higher energy input during the hybrid process. The width of the heat-affected zone for the TIG joint was also larger than that of the MIG joint. This is attributed to the fact that TIG welding is a slow welding process; hence, heat is maintained on the workpiece for a longer time resulting in high heat input. This causes a high-temperature weld pool and slower cooling rate, resulting in a larger HAZ than the MIG welded joint. On the other

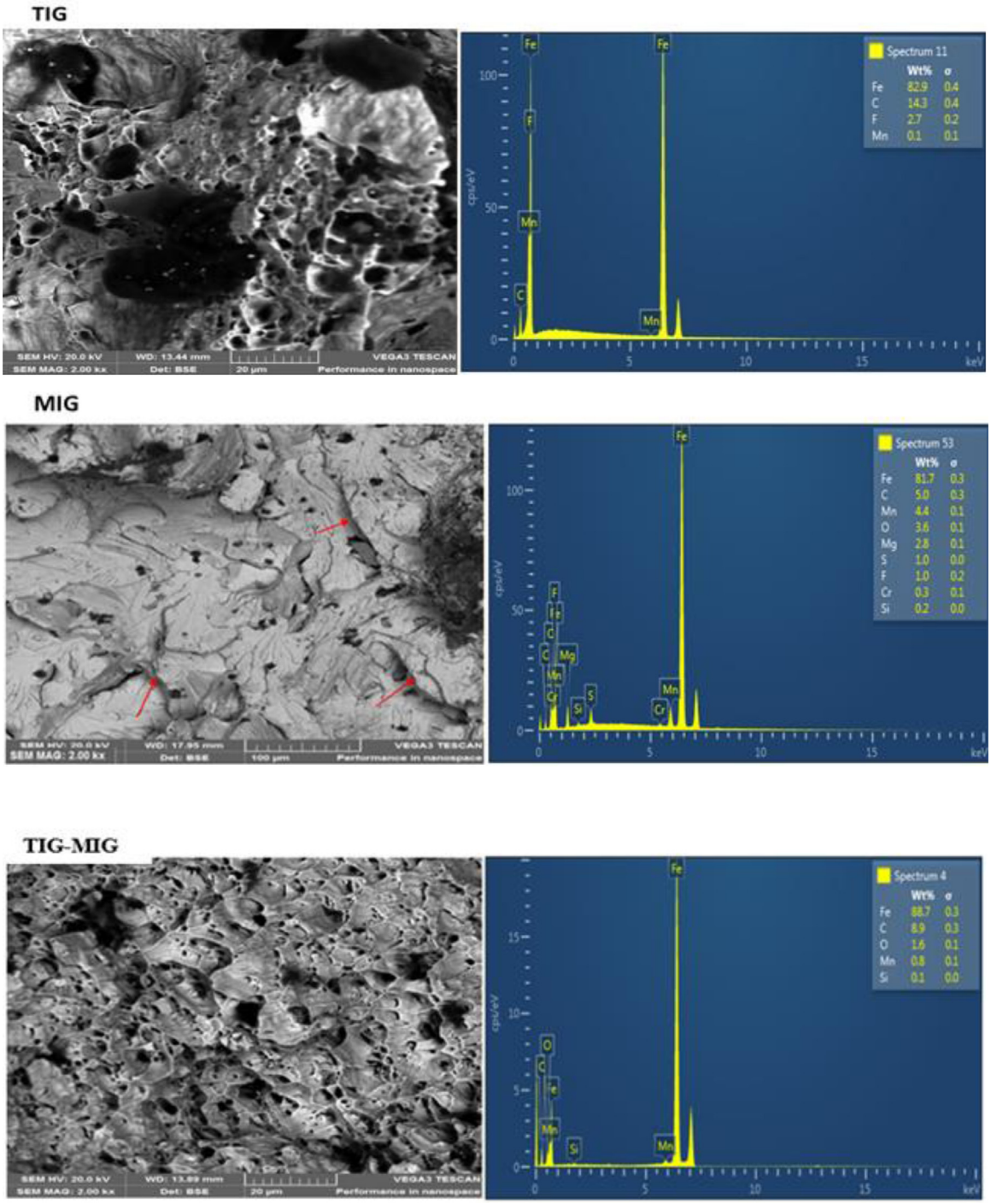

Fig. 4. Fracture morphology for the TIG, MIG and TIG-MIG hybrid welding processes.

hand, the MIG welded joint is a fast welding process. This allows for low-temperature buildup per millimetre in the weld pool resulting in faster cooling and solidification.

The microstructures of the fusion zones (FZs) and the heat-affected zones (HAZs) of the three joint types are presented (Fig. 7). The Fusion zone of the TIG welded joint is characterized by coarse dendritic cementite and lots of fine acicular ferrite, while the heat-affected zone consists of pearlite and acicular ferrite with more coarse columnar dendrite structures. The fusion zone of the MIG welded joint is characterized by Widmanstatten structures, fine acicular and proeutectoid ferrite. Sahasrabudhe and Raut [13] observed a similar structure. The HAZ of the MIG welded joint exhibited larger discrete com-

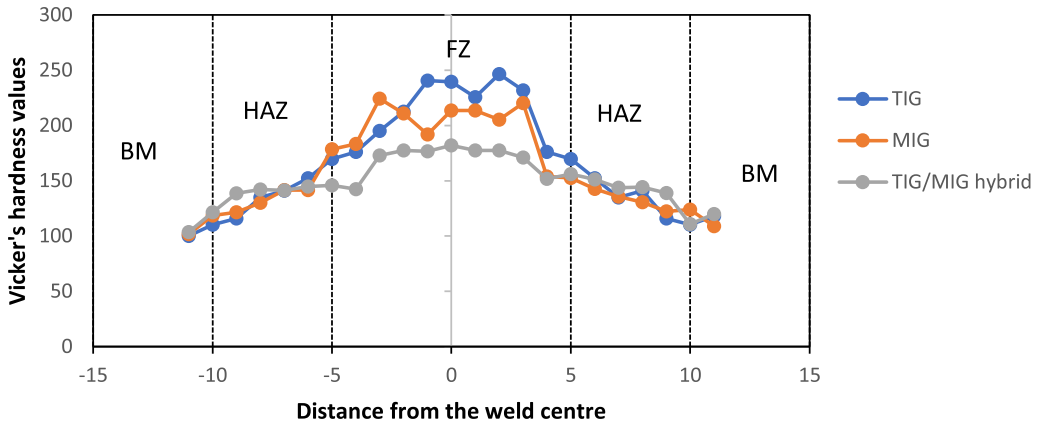

Fig. 5. Microhardness profiling for TIG, MIG and TIG-MIG hybrid joints.

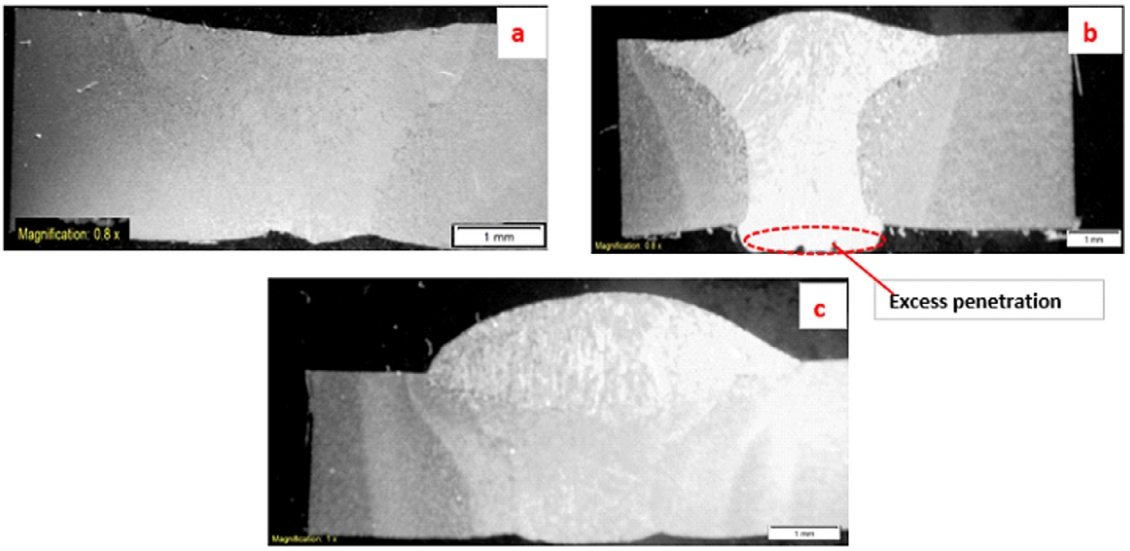

Fig. 6. Macrographs of the welded joints (a) TIG (b) MIG (c) TIG-MIG.

ponents of cementite and ferrite grains with very scanty pearlite structures. Widmanstatten ferrite formation in low carbon steel occurs due to sympathetic nucleation [16]. Sympathetic nucleation is said to occur when an alpha-ferrite nucleus is formed at the interface between a pre-existing alpha-ferrite precipitate and the parent austenite phase [17].

The microstructure of the TIG-MIG joint shows the abundant presence of acicular ferrite with cementite on the boundaries of ferrite grain. The HAZ of the TIG-MIG joint is characterized by chaotic lenticular acicular ferrite. Acicular ferrite is known to improve the strength and toughness of steel, as appraised by Loder et al. [18], Babu [19], Bahu and Bhadeshia [20], Capdevila et al. [21] and Hu et al. [22]. He and Edmonds [23] also stated that acicular ferrite is desirable in low carbon steel weldments as it improves the toughness over all other austenite transformation products. Zhao et al. [24] also affirmed that acicular ferrite microstructure in low carbon steel improved the strength and toughness. It is worthy to note that the microstructure of the TIG-MIG joint did not deteriorate despite the higher heat input value. Chen et al. [10] recorded a similar account.

XRD analysis

The diffractogram of the TIG joint is dominated by martensite phase diffracting at a peak intensity of 45.24°, 65.65° and 82.79°. However, little iron (Fe) peaks diffracted at 43.76°. The diffractogram of the MIG welded joint shows more iron phases at high-intensity peaks at 45.38° and 83.07°. Martensites phase also diffracted at a lower intensity of 65.82°. And lastly, the TIG-MIG welded joint revealed only iron phases, which accounted for its lowest hardness value. The higher

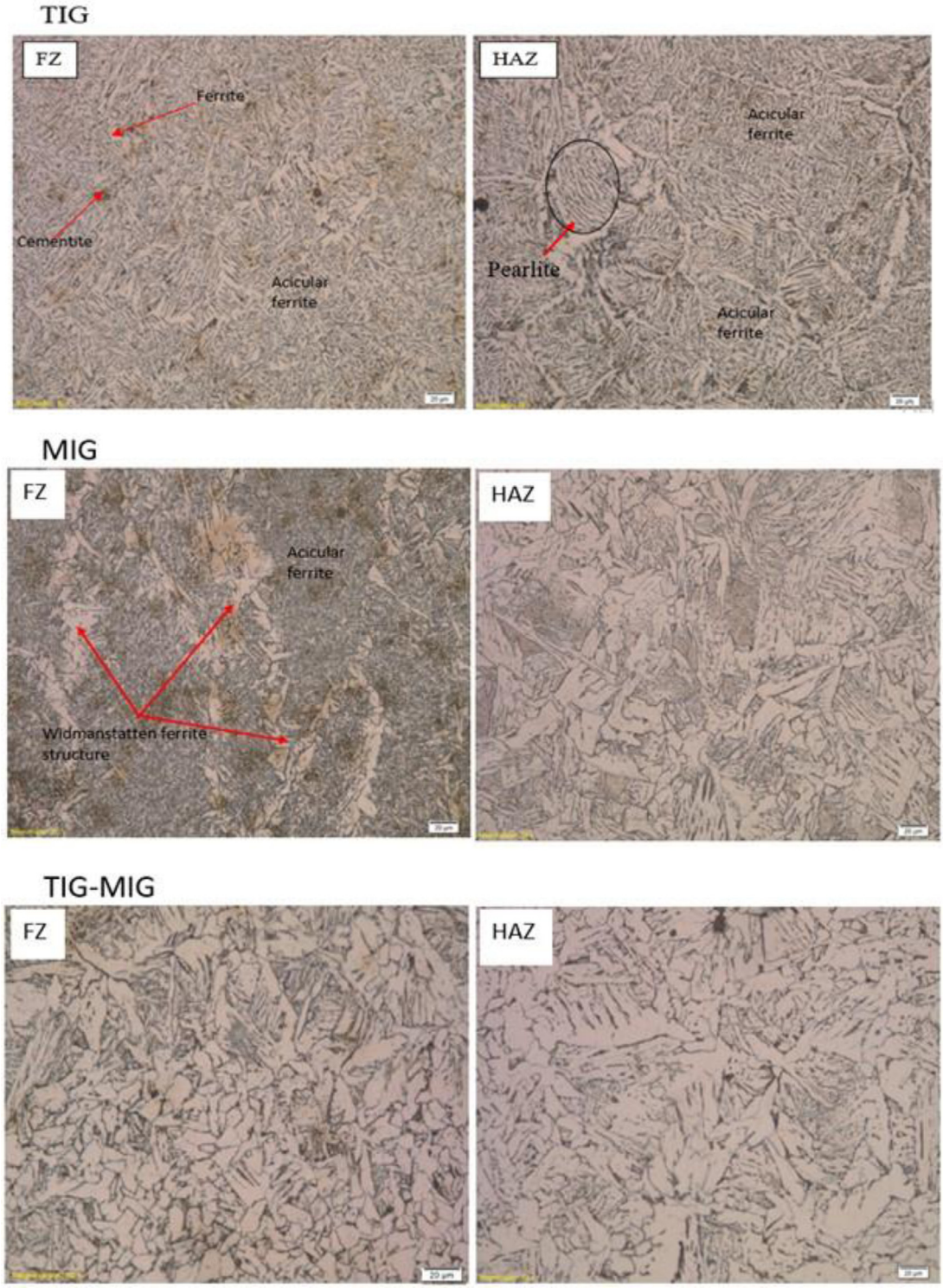

Fig. 7. Microstructures for the TIG, MIG and TIG-MIG welding processes.

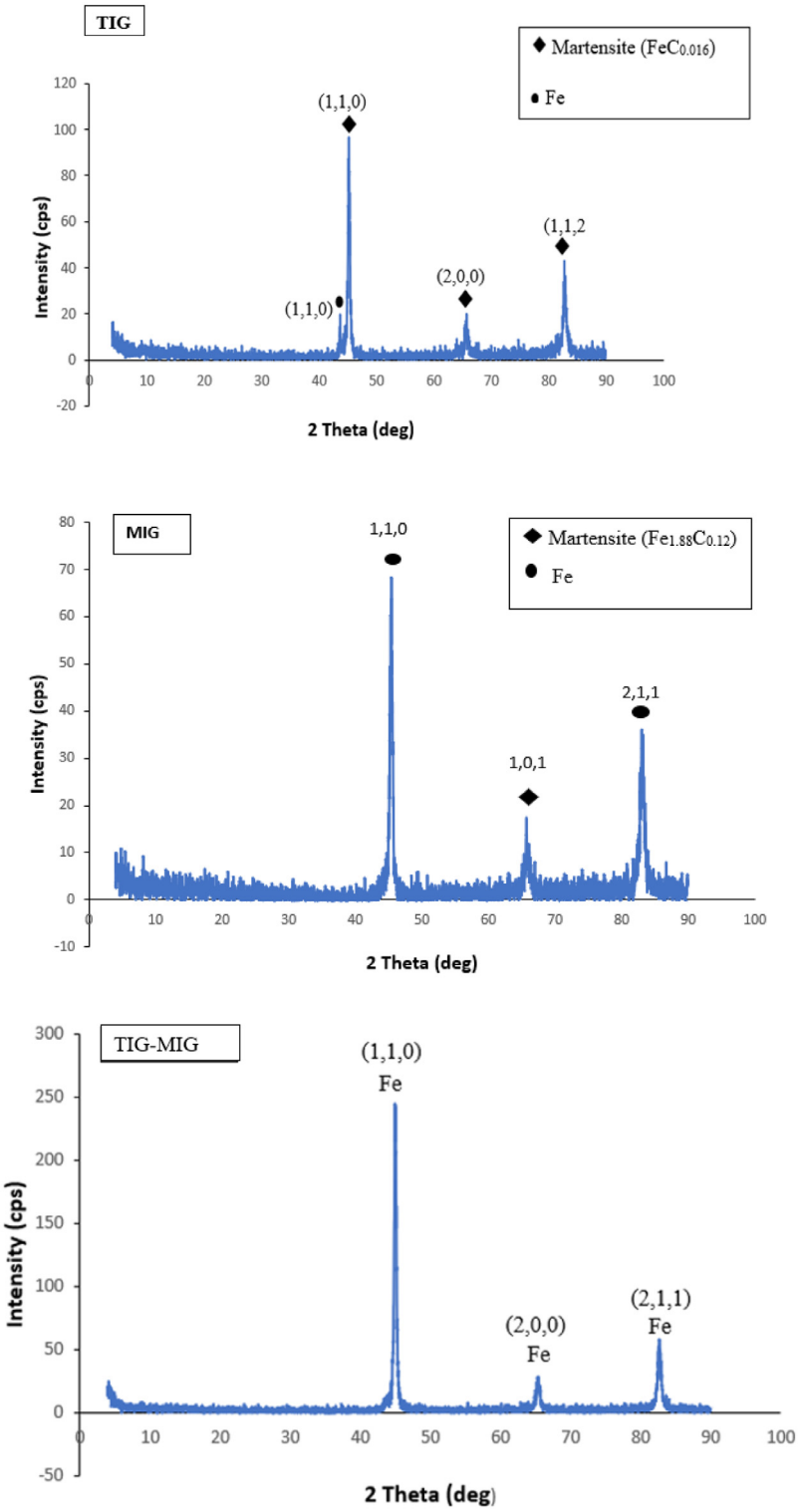

Fig. 8. The diffractogram for the TIG, MIG and TIG-MIG joints.

hardness values of the TIG and MIG joints are attributed to the presence of martensite phases. A similar observation was reported by Khan et al. [25]. The diffractogram for the TIG, MIG and TIG-MIG joints are present in Fig. 8.

Conclusion

This paper reports a comparative analysis on the microstructural, macrostructual, mechanical and phase composition of the TIG-MIG, TIG, and MIG welding processes based on optimum sets of TIG and MIG welding parameters for the enhanced structural integrity of the TIG-MIG hybrid process. Optimized input parameters combinations of the standalone TIG and MIG welding processes are employed for producing the TIG-MIG joints. The main results are summarized as follows:

Full penetration joints were achieved by the TIG, MIG and TIG-MIG welding processes

The TIG-MIG hybrid joint had better tensile properties compared to the standalone MIG and TIG welded joints. The MIG welded joint showed better tensile and yield strength compared to the TIG welded joint. The fractile morphology revealed that the TIG-MIG joint underwent a more ductile failure than standalone TIG and MIG welded joints.

The TIG-MIG hybrid weld had the lowest hardness property, which explains its highest tensile and percentage elongation values. The harder the material, the less ductile it becomes, and the more likely it is to under brittle failure.

The width of the heat-affected zone of the TIG-MIG hybrid is larger than those of the TIG and MIG process due to relatively high energy input during the hybrid process.

Widmanstatten, acicular ferrite with grain boundaries cementite in the fusions zones of the three joints accounted for the improved hardness and tensile properties compared to the parent material. The microstructure and the tensile properties of the TIG-MIG joint did not deteriorate despite the higher heat input.

The higher hardness values of the TIG and MIG joints are attributed to the presence of martensite phases.

Declaration of Competing Interest

The authors declare that they have no known competing financial interests or personal relationships that could have appeared to influence the work reported in this paper.

References

[1] G. Qin, X. Meng, B. Fu, High speed tandem gas tungsten arc welding process of thin stainless steel plate, J. Mater. Process. Technol. 220 (2015) 58–64, doi:10.1016/j.jmatprotec.2015.01.011.
[2] D. Chen, M. Chen, C. Wu, Effects of phase difference on the behavior of arc and weld pool in tandem P-GMAW, J. Mater. Process. Technol. 225 (2015) 45–55, doi:10.1016/j.jmatprotec.2015.05.022.
[3] S. Kanemaru, T. Sasaki, T. Sato, H. Mishima, S. Tashiro, M. Tanaka, Study for TIG-MIG hybrid welding process, Weld. World 58 (1) (2014) 11–18, doi:10.1007/s40194-013-0090-y.
[4] Y.Bin Zhou, D.S. Fang, L.M Liu, Root welding of V-groove thick plate without backing plate by MAG-TIG double-arc welding, Int. J. Precis. Eng. Manuf. 18 (4) (2017) 623–628, doi:10.1007/s12541-017-0074-8.
[5] R. Zong, J. Chen, C. Wu, A comparison of TIG-MIG hybrid welding with conventional MIG welding in the behaviors of arc, droplet and weld pool, J. Mater. Process. Tech. 270 (2019) 345–355 March, doi:10.1016/j.jmatprotec.2019.03.003.
[6] S. Kanemaru, T. Sasaki, T. Sato, T. Era, M. Tanaka, Study for the mechanism of TIG-MIG hybrid welding process, Weld. World 59 (2) (2015) 261–268, doi:10.1007/s40194-014-0205-0.
[7] M. Ding, S.S. Liu, Y. Zheng, Y.C. Wang, H. Li, W.Q. Xing, … P. Dong, TIG-MIG hybrid welding of ferritic stainless steels and magnesium alloys with Cu interlayer of different thickness, Mater. Des. 88 (2015) 375–383, doi:10.1016/j.matdes.2015.09.022.
[8] Z. Cheng, H. Liu, J. Huang, Z. Ye, J. Yang, S. Chen, MIG-TIG double-sided arc welding of copper-stainless steel using different filler metals, J. Manuf. Process. 55 (March) (2020) 208–219, doi:10.1016/j.jmapro.2020.04.013.
[9] Z. Ye, J. Huang, W. Gao, Y. Zhang, Z. Cheng, S. Chen, J. Yang, Microstructure and mechanical properties of 5052 aluminum alloy/mild steel butt joint achieved by MIG-TIG double-sided arc welding-brazing, Mater. Des. 123 (2017) 69–79, doi:10.1016/j.matdes.2017.03.039.
[10] J. Chen, R. Zong, C. Wu, G.K. Padhy, Q. Hu, Influence of low current auxiliary TIG arc on high speed TIG-MIG hybrid welding, J. Mater. Process. Technol. 243 (2017) 131–142, doi:10.1016/j.jmatprotec.2016.12.012.
[11] Y. Zhang, J. Huang, Z. Ye, Z. Cheng, An investigation on butt joints of Ti6Al4V and 5A06 using MIG /TIG double-side arc welding-brazing, J. Manuf. Process. 27 (2017) 221–225, doi:10.1016/j.jmapro.2017.05.010.
[12] A.A.L Ismail, M.S. Fuhaid, R.V Murali, An Experimental Analysis on Mechanical Integrity of TIG-MIG Hybrid Weldments, Int. J. Mech. Product. Eng. 5 (4) (2017) 114–117.
[13] O.S. Sahasrabudhe, D.N. Raut, Benchmarking of hybrid TIG-MAG arc welding for mild steel, Trans. Indian Inst. Met. 72 (3) (2019) 801–810, doi:10.1007/s12666-018-1536-0.
[14] X. Meng, G. Qin, Y. Zhang, B. Fu, Z. Zou, High speed TIG-MAG hybrid arc welding of mild steel plate, J. Mater. Process. Technol. 214 (11) (2014) 2417–2424, doi:10.1016/j.jmatprotec.2014.05.020.
[15] M.P. Prabakaran, G.R. Kannan, Optimization of laser welding process parameters in dissimilar joint of stainless steel AISI316/AISI1018 low carbon steel to attain the maximum level of mechanical properties through PWHT, Opt. Laser Technol. 112 (2019) 314–322, doi:10.1016/j.optlastec.2018.11.035.
[16] H.I. Aaronson, G. Spanos, R.A. Masamura, R.G. Vardiman, D.W. Moon, E.S.K. Menon, M.G. Hall, Sympathetic nucleation : an overview, Mater. Sci. Eng. B 32 (1995) 107–123.
[17] D. Phelan, R. Dippenaar, Widmanstatten ferrite plate formation in low-carbon steels, Metall. Mater. Transact. A 35 (12) (2004) 3701–3706.
[18] D. Loder, S.K. Michelic, C. Bernhard, Acicular ferrite formation and its influencing factors - a review, J. Mater. Sci. Res. 6 (1) (2017) 24–43, doi:10.5539/jmsr.v6n1p24.
[19] S.S. Babu, The mechanism of acicular ferrite in weld deposits, Curr. Opin. Solid State Mater. Sci. 8 (2004) 267–278, doi:10.1016/j.cossms.2004.10.001.
[20] S.S. Babu, H.K.D.H. Bhadeshia, Mechanism of the transition from bainite to acicular ferrite, Mater. Trans. 32 (8) (1991) 679–688.
[21] C. Capdevila, C. García-Mateo, J. Chao, F.G. Caballero, Effect of V and N precipitation on acicular ferrite formation in sulfur-lean vanadium steels, Metall. Mater. Trans. A 40 (3) (2009) 522–538, doi:10.1007/s11661-008-9730-z.
[22] J. Hu, L.X. Du, M. Zang, S.J. Yin, Y.G. Wang, X.Y. Qi, … R.D.K. Misra, On the determining role of acicular ferrite in V-N microalloyed steel in increasing strength-toughness combination, Mater. Charact. 118 (2016) 446–453, doi:10.1016/j.matchar.2016.06.027.

[23] K. He, D.V. Edmonds, Formation of acicular ferrite and influence of vanadium alloying, Mater. Sci. Technol. 18 (3) (2002) 289–296, doi:10.1179/026708301225000743.
[24] M.C. Zhao, K. Yang, Y.Y. Shan, Comparison on strength and toughness behaviors of microalloyed pipeline steels with acicular ferrite and ultrafine ferrite, Mater. Lett. 57 (9–10) (2003) 1496–1500, doi:10.1016/S0167-577X(02)01013-3.
[25] U.N. Khan, S.K. Rajput, V. Gupta, V. Verma, T. Soota, To study mechanical properties and microstructures of MIG welded high strength low alloy steel, in: In *Materials Today: Proceedings*, 18, Elsevier Ltd, 2019, pp. 2550–2555, doi:10.1016/j.matpr.2019.07.112.